

# Nonlocal nucleon-nucleus interactions in $(d, p)$ reactions: Role of the deuteron $D$ -state

G. W. Bailey, N. K. Timofeyuk, and J. A. Tostevin

*Department of Physics, Faculty of Engineering and Physical Sciences,  
University of Surrey Guildford, Surrey GU2 7XH, United Kingdom*

(Dated: March 24, 2021)

Theoretical models of the  $(d, p)$  reaction are exploited for both nuclear astrophysics and spectroscopic studies in nuclear physics. Usually, these reaction models use local optical model potentials to describe the nucleon- and deuteron-target interactions. Within such a framework the importance of the deuteron  $D$ -state in low-energy reactions is normally associated with spin observables and tensor polarization effects - with very minimal influence on differential cross sections. In contrast, recent work that includes the inherent nonlocality of the nucleon optical model potentials in the Johnson-Tandy adiabatic-model description of the  $(d, p)$  transition amplitude, which accounts for deuteron break-up effects, shows sensitivity of the reaction to the large  $n$ - $p$  relative momentum content of the deuteron wave function. The dominance of the deuteron  $D$ -state component at such high momenta leads to significant sensitivity of calculated  $(d, p)$  cross sections and deduced spectroscopic factors to the choice of deuteron wave function [Phys. Rev. Lett. **117**, 162502 (2016)]. We present details of the Johnson-Tandy adiabatic model of the  $(d, p)$  transfer reaction generalized to include the deuteron  $D$ -state in the presence of nonlocal nucleon-target interactions. We present exact calculations in this model and compare these to approximate (leading-order) solutions. The latter, approximate solutions can be interpreted in terms of local optical potentials, but evaluated at a shifted value of the energy in the nucleon-target system. This energy shift is increased when including the  $D$ -state contribution. We also study the expected dependence of the  $D$ -state effects on the separation energy and orbital angular momentum of the transferred nucleon. Their influence on the spectroscopic information extracted from  $(d, p)$  reactions is quantified for a particular case of astrophysical significance.

## I. INTRODUCTION

A primary interest in  $(d, p)$  reactions, especially those studied at modern radioactive beam facilities, is their ability to reveal single-particle spectra of rare isotopes and to determine the angular momentum content and spectroscopic strength of single-particle states near their Fermi-surfaces. This information is crucial also in nuclear astrophysics applications. These angular momenta and associated spectroscopic strengths are deduced from comparisons of the measured cross sections with theoretical predictions. Differences between theoretical models of the reaction thus impact the interpretation of experimental data and studies of the sensitivities of calculations to model assumptions are vital.

Necessary inputs to direct reaction models of the  $A(d, p)B$  transfer process, such as the distorted-waves Born approximation (DWBA) [1] and adiabatic distorted-waves approximation (ADWA) [2] methods, are complex effective interactions (optical potentials) between the reactants in the entrance ( $d - A$ ) and exit ( $p - B$ ) channels. Feshbach theory clarifies that these interactions should be both complex and nonlocal, arising from the many-body nature of the nuclei  $A$  and  $B$  and the effects of inelastic channel couplings upon the elastic channel wave functions [3]. Within the DWBA, taking account of nonlocalities of the Perey-Buck type [4] results in a multiplication of the entrance and exit channel distorted waves by a *Perey factor* [5]. However, the DWBA neglects important contributions due to transfer from the deuteron breakup continuum that require a consideration of the nucleon-target degrees of freedom in the entrance

channel. These deuteron breakup effects are treated efficiently in the ADWA method [2], that develops the  $d - A$  effective potential from those of the  $n - A$  and  $p - A$  systems. Until very recently, these  $n - A$  and  $p - A$  optical potentials used to describe the  $n + p + A$  entrance channel were assumed to be local. In the ADWA, nonlocality in the proton (exit) channel can be included in the same manner as in the DWBA. This proton channel nonlocality has been treated exactly in recent calculations [6, 7]. However, constructing the  $d - A$  effective potentials when including nonlocal nucleon-target ( $N - A$ ) potentials required additional formal developments, as presented only relatively recently [8–11]. In addition, earlier work that included  $N - A$  nonlocalities using Faddeev framework three-body calculations showed an improved description of  $(d, p)$  reaction cross sections on a range of closed-shell targets [12].

It was shown in Refs. [8, 9] that including nonlocal  $p - A$  and  $n - A$  potentials in the adiabatic model of the  $A(d, p)B$  reaction generates a nonlocal adiabatic  $d - A$  potential. This model could be further reduced, to a local one, in a similar way to that originally introduced by Perey and Buck [4]. This revised local adiabatic potential  $U_{dA}^{\text{loc}}$  is different to that which is usually constructed in the ADWA method, that uses energy-dependent phenomenological local nucleon optical potentials and then evaluates these at half the energy of the incident deuteron,  $E_d$ . Instead, Refs. [8, 9] show, for  $Z = N$  targets, that  $U_{dA}^{\text{loc}}$  should be constructed from nucleon optical potentials evaluated at a shifted energy  $E = E_d/2 + \Delta E$ . The required shift,  $\Delta E$ , is related to the value of  $\langle T_{np} \rangle_V$ , a measure of the  $n - p$  relative ki-

netic energy  $T_{np}$  in the deuteron ground-state  $\phi_0$  inside the range of the  $n-p$  interaction,  $V_{np}$ , that binds the deuteron. Specifically, this value is

$$\langle T_{np} \rangle_V = \frac{\langle \phi_0 | V_{np} T_{np} | \phi_0 \rangle}{\langle \phi_0 | V_{np} | \phi_0 \rangle} \equiv \langle \phi_1 | T_{np} | \phi_0 \rangle, \quad (1)$$

where we have defined

$$|\phi_1\rangle = V_{np}|\phi_0\rangle / \langle \phi_0 | V_{np} | \phi_0 \rangle. \quad (2)$$

Given the short-range nature of the nucleon-nucleon (NN) interaction and  $\phi_1$ , a major contribution to  $\langle T_{np} \rangle_V$  arises from high  $n-p$  relative momenta.

In Ref. [9], values of  $\langle T_{np} \rangle_V$  and  $\Delta E$  were obtained assuming the  $S$ -state wave function of the purely attractive, phenomenological central NN interaction of Hulthén [13], whereas realistic deuteron wave functions have a modest  $D$ -state component with probability  $P_D \approx 4-7\%$ . Though modest, this  $D$ -state component can dominate the wave function at high  $n-p$  momenta with important implications for calculations of  $U_{dA}^{\text{loc}}$  and  $(d,p)$  cross sections. The intrinsic nonlocality of optical potentials thus presents a distinct and novel source of  $D$ -state and  $n-p$  momentum sensitivity of cross sections for such reactions. This is in contrast with previous  $D$ -state studies, e.g. [14, 15], that focused on the effects of the  $D$ -state component of the reaction vertex  $V_{np}|\phi_0\rangle$  in the DWBA amplitude. The conclusions there, for low energy reactions, are that DWBA cross sections and vector analysing powers are insensitive to the deuteron  $D$ -state, the primary sensitivity being on the tensor polarization observables.

In this paper we develop exact adiabatic model  $(d,p)$  reaction calculations that use energy-independent non-local nucleon optical potentials and that include the deuteron  $D$ -state. We derive formal expressions and calculate the nonlocal deuteron channel potential  $U_{dA}$  and the corresponding  $d-A$  distorted waves. The effects on  $(d,p)$  cross sections are discussed and compared with those obtained from the earlier, approximate lowest-order local model. Our key findings, applied to a  $^{26}\text{Al}$  target, were presented in Ref. [16] and focused on the sensitivity of  $\langle T_{np} \rangle_V$  and the corresponding  $(d,p)$  cross sections to high  $n-p$  momenta, which is different between NN models. It was shown that, in some cases, cross sections can change significantly with different choices of deuteron wave function, and that these changes correlate with the  $D$ -state component. Here, we present full details of the model calculations and extend the model's application to include  $^{40}\text{Ca}$  and  $^{28}\text{Si}$  targets. For  $^{28}\text{Si}$  we explore a range of neutron separation energies and different orbital angular momentum transfers. We restrict ourselves to low-energy  $(d,p)$  reactions, relevant to ISOL facilities, where spin-orbit terms of the nucleon optical potentials and finite-range effects of the transition interaction can be neglected, allowing a clearer evaluation of the  $D$ -state effects.

In Sec. II we review the role of the  $D$ -state on the  $d-A$  distorted wave and cross sections within the standard (local) ADWA and in the DWBA with the Watanabe folding

model  $d-A$  potential. In Sec. III we then present the formalism for the nonlocal deuteron adiabatic potential. In Sec. IV we compare the present results, made in a lowest-order approximation, to those obtained in the local model proposed in Refs. [8, 9]. In Sec. V we present the present exact calculations for several targets, focusing on how  $D$ -state effects evolve with the separation energy and orbital angular momentum of the transferred neutron. Implications for extracted spectroscopic factors are discussed for a specific reaction of astrophysical interest, on a  $^{26}\text{Al}$  target. Conclusions are drawn in Sec. VI. Other relevant details are presented in an Appendix.

## II. D-STATE IN ADWA WITH LOCAL NUCLEON OPTICAL POTENTIALS

Before presenting our nonlocal potential plus  $D$ -state  $(d,p)$  model we comment on  $D$ -state contributions to standard local ADWA calculations. The ADWA includes deuteron break up effects through a three-body ( $A+n+p$ ) description of the deuteron channel. The  $(d,p)$  transition amplitude in the three-body model is

$$T_{(d,p)} = \sqrt{C^2 S} \langle \chi_p^{(-)} \phi_n | V_{np} | \Psi_d^{(+)} \rangle, \quad (3)$$

where  $\Psi_d^{(+)}(\mathbf{R}, \mathbf{r})$  is the deuteron channel three-body wave function,  $\mathbf{R}$  is the vector separation of the deuteron and the target,  $\mathbf{r}$  the neutron-proton separation and  $V_{np}$  is the neutron-proton interaction in the deuteron. Following the convention used in Ref. [9], we define  $\mathbf{r} = \mathbf{r}_n - \mathbf{r}_p$  and  $\mathbf{R} = -(\mathbf{r}_n + \mathbf{r}_p)/2$  where  $\mathbf{r}_n$  and  $\mathbf{r}_p$  are the positions of the incident neutron and proton relative to the mass  $A$  target. Thus, with this convention,  $\mathbf{r}_n = \mathbf{r}/2 - \mathbf{R}$  and  $\mathbf{r}_p = -\mathbf{r}/2 - \mathbf{R}$ . In the final state, the proton channel distorted wave  $\chi_p^{(-)}$  is a function of  $\mathbf{R}_p$ , the position of the outgoing proton relative to the product nucleus  $B(=A+n)$ .  $\phi_n$  is the normalised bound-state wave function of the transferred neutron in the final state (more generally, the neutron overlap function) and  $C^2 S$  is its spectroscopic factor.

The ADWA makes use of a Weinberg states expansion of  $\Psi_d^{(+)}$  [2], valid for  $\mathbf{r}$  values within the range of  $V_{np}$ , as required to evaluate  $T_{(d,p)}$ . It was shown [17] that with this basis, the transition amplitude converges rapidly and only the first Weinberg state needs to be retained. With this approximation  $\Psi_d^{(+)}(\mathbf{R}, \mathbf{r}) \rightarrow \chi_d^{(+)}(\mathbf{R})\phi_0(\mathbf{r})$  and  $T_{(d,p)}$  in the ADWA is

$$T_{(d,p)} = \sqrt{C^2 S} \langle \chi_p^{(-)} \phi_n | V_{np} | \chi_d^{(+)} \phi_0 \rangle, \quad (4)$$

where  $\chi_d^{(+)}(\mathbf{R})$  describes the center-of-mass distortion of the incident  $np$ -pair in the presence of deuteron breakup effects. When the nucleon-target potentials  $U_{NA}$  ( $N = n, p$ ) are local,  $\chi_d^{(+)}(\mathbf{R})$  is calculated from the adiabatic distorting potential

$$U_{dA} = \langle \phi_1 | U_{pA}(-\mathbf{r}/2 - \mathbf{R}) + U_{nA}(\mathbf{r}/2 - \mathbf{R}) | \phi_0 \rangle. \quad (5)$$

Because of the short range of  $\phi_1$ , of Eq. (2), the main contributions in Eq. (5) come from values  $r \approx 0$ . Letting  $r \rightarrow 0$  connects the Weinberg states technique and the earlier Johnson-Soper adiabatic formalism where, assuming a zero-range  $V_{np}$ ,  $U_{dA}^{JS}(R) = U_{nA}(R) + U_{pA}(R)$  [18] and, in which limit, the adiabatic potential is seen to be independent of details of the assumed deuteron wave function. As is now shown, full calculations of the central terms of  $U_{dA}$  of Eq. (5), with different realistic deuteron wave functions and local nucleon-target interactions, give very similar results and show essentially no sensitivity to the  $D$ -state.

Below we show  $U_{dA}$  for the deuteron wave function of the Argonne  $V_{18}$  (AV18) NN interaction [19], with both  $S$ - and  $D$ -state components. In the presence of the  $D$ -state, we write the deuteron ground state wave function  $\phi_0^{M_d}$ , with angular momentum projection  $M_d$ , as

$$\phi_0^{M_d}(\mathbf{r}) = \sum_{l_d \lambda_d s_d \sigma_d} (l_d \lambda_d s_d \sigma_d | J_d M_d) \frac{u_{l_d}(r)}{r} Y_{l_d}^{\lambda_d}(\hat{\mathbf{r}}) \chi_{s_d}^{\sigma_d}, \quad (6)$$

with  $l_d \lambda_d, s_d \sigma_d$  the orbital and spin angular momenta and their projections coupled to  $J_d (= 1)$ ,  $\chi$  is the  $np$  spinor and the  $u_{l_d}(r)$  are the deuteron  $S$ - and  $D$ -state radial wave functions. The vertex function  $V_{np} \phi_0^{M_d}$  has an identical form but with the  $u_{l_d}(r)$  replaced by short-ranged radial vertex functions  $v_{l_d}(r)$ .

The calculated adiabatic potential  $U_{dA}$  for the  $d$ - $^{40}\text{Ca}$  system at  $E_d = 10$  MeV, using the Chapel Hill 89 (CH89) phenomenological local optical potential for the  $U_{NA}$  [20], is shown in Fig. 1a. For comparison, the  $U_{dA}$  calculated using the  $S$ -state Hulthén wave function is also shown. The two potentials are very similar, as are the corresponding  $^{40}\text{Ca}(d, p)^{41}\text{Ca}$  cross sections, presented in Fig. 1b. All of the NN potential models used in Ref. [16] lead to this same conclusion. We add that there is also negligible  $D$ -state sensitivity in the central terms of the deuteron-target interaction and the transfer reaction cross sections in the no-breakup limit of the  $d - A$  scattering - the Watanabe folding model [21] - when the distorting potential is

$$U_{dA}^{\text{Wat}} = \langle \phi_0 | U_{pA}(-\mathbf{r}/2 - \mathbf{R}) + U_{nA}(\mathbf{r}/2 - \mathbf{R}) | \phi_0 \rangle. \quad (7)$$

The calculated Watanabe potentials are also shown in Fig. 1a for both the Hulthén and AV18 cases. The  $D$ -state and NN-model insensitivity of the corresponding (DWBA) cross sections is shown in Fig. 1b.

In the cross section calculations above, and throughout this paper, we use the zero-range approximation,  $D(\mathbf{r}) = \langle \mathbf{r} | V_{np} | \phi_0 \rangle \approx D_0 \delta(\mathbf{r})$  to the transition interaction when calculating  $T_{(d,p)}$ . The volume integrals  $D_0$  are determined for each NN model, and are given in Table I for the models used here. The zero-range approximation to  $T_{(d,p)}$  is very accurate for reactions of low energy deuteron beams, where finite-range corrections are small, e.g. [22]. Hence, we compute the transition amplitudes

$$T_{(d,p)} = D_0 \sqrt{C^2 S} \langle \chi_p^{(-)} | \phi_n | \chi_d^{(+)} \rangle. \quad (8)$$

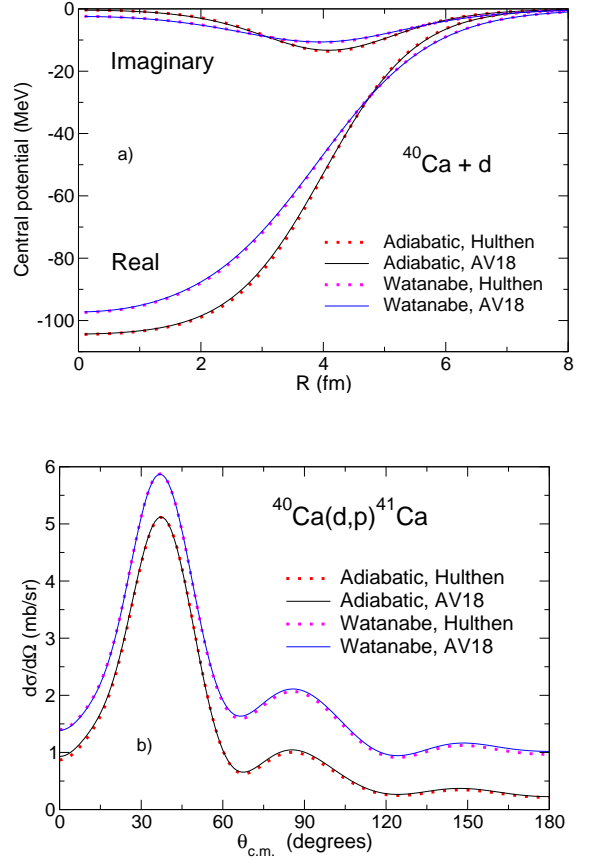


FIG. 1. (a) Adiabatic and Watanabe potentials for  $d$ - $^{40}\text{Ca}$  at  $E_d = 10$  MeV, and (b)  $^{40}\text{Ca}(d, p)^{41}\text{Ca}$  differential cross sections for  $E_d = 10$  MeV, using the Chapel Hill 89 phenomenological local optical potential for two NN potential models: (i) the central Hulthén potential with an  $S$ -state deuteron (dots) and (ii) the realistic AV18 potential and deuteron with both the  $S$ - and  $D$ -states (solid lines).

In the following we calculate  $T_{(d,p)}$  when both  $\chi_p^{(-)}$  and  $\chi_d^{(+)}$  are generated by nonlocal potential models - the latter including realistic deuteron wave functions and  $D$ -state effects through the adiabatic model entrance channel effective interaction.

### III. THE NONLOCAL SCATTERING PROBLEM

In this section we describe the computations of the distorted waves  $\chi_p^{(-)}$  and  $\chi_d^{(+)}$  for the ADWA calculations in the nonlocal model case. They satisfy the inhomogeneous Schrödinger-like equation, with  $\alpha = p$  or  $d$ ,

$$(T_\alpha + U_c(R) - E) \chi_\alpha(\mathbf{R}) = - \int d\mathbf{R}' U_\alpha(\mathbf{R}, \mathbf{R}') \chi_\alpha(\mathbf{R}'), \quad (9)$$

where  $E$ ,  $T_\alpha$  and  $U_c$  are the center of mass energy, kinetic energy operator and Coulomb interaction and  $U_\alpha(\mathbf{R}, \mathbf{R}')$

is the nonlocal nuclear potential in channel  $\alpha$ . Throughout this work we adopt an energy-independent Perey-Buck parameterization of the nonlocal nucleon-target potentials. Equation (9) is solved iteratively, following partial wave decomposition, from a trial complex and local starting potential  $U_\alpha(R)$ , namely

$$(T_\alpha + U_\alpha(R) + U_c(R) - E)\chi_\alpha^{(i+1)}(\mathbf{R}) = - \int d\mathbf{R}' [\mathcal{U}_\alpha(\mathbf{R}, \mathbf{R}') - U_\alpha(R)\delta(\mathbf{R} - \mathbf{R}')] \chi_\alpha^{(i)}(\mathbf{R}')$$

with  $\chi_\alpha^{(0)}$  the solution of the homogeneous equation with the appropriate scattering boundary conditions. Our treatment of the proton and deuteron channel nonlocal potentials is described in detail below.

### A. Proton Channel

The nonlocal interaction in the proton channel describes the motion of the outgoing proton with respect to the resultant nucleus  $B(=A+n)$ . This is of Perey-Buck type, i.e.

$$\mathcal{U}_{pA}(\mathbf{R}_p, \mathbf{R}'_p) = H(|\mathbf{R}_p - \mathbf{R}'_p|) U_{pA} \left( \frac{|\mathbf{R}_p + \mathbf{R}'_p|}{2} \right), \quad (10)$$

with  $H$  a normalized Gaussian (in 3 dimensions) with a range  $\beta$ ,

$$H(x) = (\sqrt{\pi}\beta)^{-3} \exp(-x^2/\beta^2). \quad (11)$$

The potential form factors  $U_{NA}$  are complex with conventional Woods-Saxon real parts and surface-peaked derivative Woods-Saxon imaginary parts. This nonlocal interaction is used directly in the source term of the inhomogeneous equation, Eq. (9). Thus, the proton channel partial wave functions  $\chi_L^J$ , with  $\mathbf{J} = \mathbf{L} + \mathbf{s}_p$ ,  $s_p = 1/2$ , satisfy

$$\begin{aligned} (T_p^{(L)} + U_c(R_p) - E_p) \chi_L^J(R_p) = \\ - R_p \int_0^\infty dR'_p R'_p \mathcal{U}_L^{(p)}(R_p, R'_p) \chi_L^J(R'_p) \end{aligned} \quad (12)$$

with

$$T_\alpha^{(L)} = -\frac{\hbar^2}{2m_\alpha} \left[ \frac{d^2}{dR_\alpha^2} - \frac{L(L+1)}{R_\alpha^2} \right] \quad (13)$$

and  $m_\alpha$  is the reduced mass in channel  $\alpha$ . The potential kernel is

$$\begin{aligned} \mathcal{U}_L^{(p)}(R_p, R'_p) = 2\pi \int_{-1}^1 d\mu P_L(\mu) H(|\mathbf{R}_p - \mathbf{R}'_p|) \\ \times U_{pA} \left( \frac{|\mathbf{R}_p + \mathbf{R}'_p|}{2} \right), \end{aligned} \quad (14)$$

where  $\mu = \mathbf{R}_p \cdot \mathbf{R}'_p / R_p R'_p$  and  $P_L$  is the Legendre polynomial of order  $L$ . With the neglect of spin-orbit interactions, as assumed here, the  $J = L \pm 1/2$  channel distorted waves are of course identical.

In all of the nonlocal ADWA calculations presented, the exact solutions of Eq. (12) are read into the transfer reactions code TWOFNR [23]. Comparisons between such exact solutions and those from a phase-equivalent model can be found in Ref. [6].

### B. Deuteron Channel

The nonlocal deuteron channel potential  $\mathcal{U}_{dA}(\mathbf{R}, \mathbf{R}')$  is constructed using nonlocal nucleon-target optical potentials with the Perey-Buck form of Eq. (10). The formal expression for the Johnson-Tandy adiabatic model potential  $\mathcal{U}_{dA}(\mathbf{R}, \mathbf{R}')$  in terms of the nucleon potentials  $\mathcal{U}_{NA}(\mathbf{R}_N, \mathbf{R}'_N)$  is given by Eq. (12) of Ref. [9] - a folding-type integral where the arguments of the nucleon optical potentials are reexpressed in terms of the deuteron channel variables  $\mathbf{R}$ ,  $\mathbf{R}'$  and  $\mathbf{r}$ . Here, we take the target mass  $A$  to be infinitely large in the more general expression of Ref.[9]. The partial wave form of  $\mathcal{U}_{dA}(\mathbf{R}, \mathbf{R}')$  is more complicated when the  $D$ -state is present and the required expansion is most easily achieved by use of the variables  $\mathbf{R}$  and  $\mathbf{S} = \mathbf{R} - \mathbf{R}'$ . We obtain

$$\begin{aligned} \mathcal{U}_{dA}^{M_d M'_d}(\mathbf{R}, \mathbf{S}) = 8H(2\mathbf{S}) \int d\mathbf{x} \phi_1^{*M_d}(\mathbf{x} - 2\mathbf{S}) \\ \times \left[ U_{nA}(\frac{\mathbf{x}}{2} - \mathbf{R}) + U_{pA}(\frac{\mathbf{x}}{2} - \mathbf{R}) \right] \phi_0^{M'_d}(\mathbf{x}), \end{aligned} \quad (15)$$

where  $M_d, M'_d$  are the projections of the intrinsic angular momentum  $J_d (=1)$  of the deuteron referred to the incident beam direction.

We multipole expand the vertex function  $\phi_1$  and the nonlocal nucleon-target potential formfactors in terms of the vectors  $\mathbf{x}$ ,  $\mathbf{S}$  and  $\mathbf{R}$ , and separate their radial and angular components. After summation over angular momentum projections,  $\mathcal{U}_{dA}$  is the operator in deuteron spin space

$$\begin{aligned} \mathcal{U}_{dA}(\mathbf{R}, \mathbf{S}) = 4\pi \sum_{l_1 l_2 a} v_{l_1 l_2}^a(R, S) \sum_{\alpha} (-1)^{a-\alpha} \mathcal{T}_{a-\alpha} \\ \times \left[ Y_{l_1}(\hat{\mathbf{R}}) \otimes Y_{l_2}(\hat{\mathbf{S}}) \right]_{a\alpha}, \end{aligned} \quad (16)$$

where  $\mathcal{T}_{kq}$  is the irreducible tensor operator of rank  $k$  in the space of spin  $J_d$  with matrix elements

$$\langle J_d M_d | \mathcal{T}_{kq} | J_d M'_d \rangle = \hat{k} \langle J_d M'_d k q | J_d M_d \rangle.$$

The functions  $v_{l_1 l_2}^a$  contain all information on the deuteron wave function and nonlocal potential form factors, details of which are presented in an Appendix. Further expansion of  $v_{l_1 l_2}^a$  and  $Y_{l_2}(\hat{\mathbf{S}})$ , now with respect to  $\mathbf{R}$  and  $\mathbf{R}'$ , then derives the required (radial variables) kernel of  $\mathcal{U}_{dA}$ ,

$$\begin{aligned}
\mathcal{U}_{L'L''}^J(R, R') = & 2\pi \sum_{al_1l_2} \sum_{\substack{\mathcal{L}\mathcal{L}' \\ \tau+\eta=l_2}} \hat{a}^2 \hat{J}_d \hat{l}_1 \hat{l}_2 \hat{\mathcal{L}}^2 \hat{\mathcal{L}}' \left[ \frac{(2l_2+1)!}{(2\tau)!(2\eta)!} \right]^{\frac{1}{2}} (\tau 0 \mathcal{L} 0 | \mathcal{L}' 0) (\eta 0 \mathcal{L} 0 | L'' 0) (l_1 0 \mathcal{L}' 0 | L' 0) W(\mathcal{L}' \mathcal{L} l_2 \eta; \tau L'') \\
& \times W(L'' \mathcal{L}' a l_1; l_2 L') W(L' a J J_d; L'' J_d) R^\tau R'^\eta \int_{-1}^1 \frac{v_{l_1 l_2}^a(R, |\mathbf{R} - \mathbf{R}'|)}{|\mathbf{R} - \mathbf{R}'|^{l_2}} P_{\mathcal{L}}(\mu) d\mu. \quad (17)
\end{aligned}$$

Here, in standard notations,  $\hat{x} = \sqrt{2x+1}$ ,  $W$  is the Racah coefficient and  $\mu = \mathbf{R} \cdot \mathbf{R}' / RR'$ . These nonlocal kernels,  $\mathcal{U}_{L'L''}^J(R, R')$ , enter the Schrödinger-like equation for the deuteron distorted waves  $\chi_{L'L}^J(R)$  for total angular momentum  $J$ . Explicitly,

$$\begin{aligned}
& (T_d^{(L')} + U_c(R) - E_d) \chi_{L'L}^J(R) \\
& = -R \sum_{L''} \int_0^\infty dR' R' \mathcal{U}_{L'L''}^J(R, R') \chi_{L''L}^J(R') \quad (18)
\end{aligned}$$

where  $T_d^{(L')}$  is given by Eq. (13).

The central terms of  $\mathcal{U}_{dA}$ , corresponding to  $a = 0$ , are of course diagonal in the orbital angular momentum quantum number and

$$\begin{aligned}
\mathcal{U}_{L'L''}^J(R, R') = & 2\pi \delta_{L'L''} \sum_{\substack{l\mathcal{L}\mathcal{L}' \\ \tau+\eta=l}} \frac{\hat{\mathcal{L}}^2 \hat{\mathcal{L}}' \hat{l}}{\hat{L}'^2} \left[ \frac{(2l+1)!}{(2\tau)!(2\eta)!} \right]^{\frac{1}{2}} \\
& \times (\tau 0 \mathcal{L} 0 | \mathcal{L}' 0) (\eta 0 \mathcal{L} 0 | L' 0) (l 0 \mathcal{L}' 0 | L' 0) W(\mathcal{L}' \mathcal{L} l \eta; \tau L') \\
& \times R^\tau R'^\eta \int_{-1}^1 \frac{v_{ll}^0(R, |\mathbf{R} - \mathbf{R}'|)}{|\mathbf{R} - \mathbf{R}'|^l} P_{\mathcal{L}}(\mu) d\mu. \quad (19)
\end{aligned}$$

The smaller potential terms with  $a = 2$ , of tensor character, arise only when the deuteron  $D$ -state is included.

#### IV. LOWEST-ORDER APPROXIMATION TO THE NONLOCAL MODEL

Before calculating these  $\mathcal{U}_{dA}$  exactly, we investigate the potential calculated in an approximation, called the lowest-order (LO) limit. Here, due to the short range of  $\phi_1$  in the folding integral, Eq. (15), we replace

$$U_{NA}(|\mathbf{x}/2 - \mathbf{R}|) \rightarrow U_{NA}(R) \quad (20)$$

as was also used in [8, 9], there assuming an  $S$ -wave deuteron. This limit calculates the leading-order contributions to the potential and the  $(d, p)$  cross section and provides insight into the nature of the derived entrance channel interaction. It was shown previously [9], in this limit and within the local-energy approximation (LEA), that the adiabatic potential is local and that this local potential,  $U_{dA}^{\text{loc}}$ , solves the transcendental equation

$$U_{dA}^{\text{loc}} = M_0 U_d(R) \exp \left[ -\frac{m_d \beta_d^2}{2\hbar^2} (E_d - U_{dA}^{\text{loc}} - U_c) \right], \quad (21)$$

where  $m_d$  is the deuteron channel reduced mass,  $\beta_d$  is the effective deuteron nonlocality range [9] and  $M_0$  is the zeroth-order moment of the nonlocality factor

$$M_0 = \int d\mathbf{s} \int d\mathbf{x} H(s) \phi_1(\mathbf{x} - \mathbf{s}) \phi_0(\mathbf{x}). \quad (22)$$

In Eq. (21) and below,  $U_d(R) = U_{nA}(R) + U_{pA}(R)$ .

Further, it was shown, for  $Z = N$  nuclei, that  $U_{dA}^{\text{loc}}$  can be constructed from phenomenological local nucleon optical potentials that describe elastic scattering at an energy shifted by  $\Delta E$  from the usually assumed value,  $E_d/2$ , of half the incident deuteron energy. Through  $M_0$ , this shift  $\Delta E$  is determined by  $\langle T_{np} \rangle_V$  of Eq. (1). Here, we find that Eq. (21) and its shifted-energy solution remain valid when a deuteron  $D$ -state is present. However, the values of  $\langle T_{np} \rangle_V$ ,  $M_0$  and  $\Delta E$  are strongly affected by the presence of the  $D$ -state component. For example, Table I shows that the  $\Delta E$  values for the neutron, from NN models with a  $D$ -state component, typically span an interval from 38–75 MeV, significantly larger than the  $\Delta E$  of 32 MeV from the  $S$ -wave Hulthén NN model.

NN Model	$P_D$ %	$D_0$ MeV fm $^{\frac{3}{2}}$	$\langle T_{np} \rangle_V$ MeV	$\Delta E$ MeV
Hulthén	0	−126.15	106.6	31.7
Reid soft core	6.46	−125.19	245.8	75.3
Argonne V18	5.76	−126.11	218.0	66.8
CD-Bonn	4.85	−126.22	112.5	37.6

TABLE I.  $D$ -state percentages  $P_D$ , volume integrals  $D_0$  of the transfer vertex  $D(\mathbf{r})$ , and short-ranged  $n$ - $p$  kinetic energy  $\langle T_{np} \rangle_V$  for different NN-model interactions used here. The neutron energy shifts  $\Delta E$  are calculated for the  $d+^{40}\text{Ca}$  system at  $E_d = 11.8$  MeV and are computed using the lowest-order methodology discussed here. The proton energy shifts are larger by the Coulomb energy,  $\approx 6.8$  MeV for  $^{40}\text{Ca} + p$  scattering. Details can be found in sections IV.A and IV.B of Ref. [9].

Below we will present, as typical, calculations for the phenomenological AV18 NN potential. The other NN potentials studied, see Table I and also Table I of Ref. [16], give both larger and smaller  $\Delta E$ . We note also that, if we include only the  $S$ -wave part of the AV18 wave function, then the values of both  $M_0$  and  $\Delta E$  are very similar to those of the Hulthén wave function. Thus, the primary difference between the AV18 and Hulthén model results arises from the  $D$ -state component of the wave function.

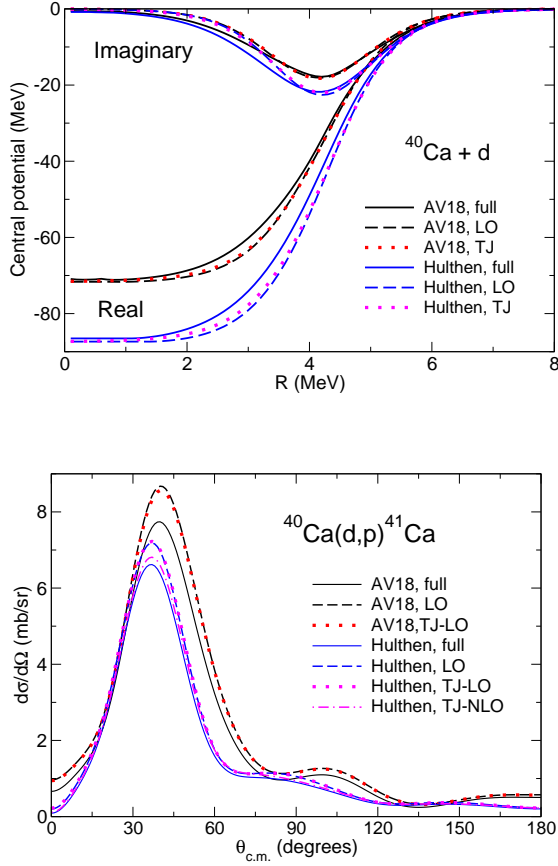


FIG. 2. (a) Trivially-equivalent local adiabatic potentials for  $d-^{40}\text{Ca}$ , and (b) the  $^{40}\text{Ca}(d,p)^{41}\text{Ca}$  differential cross sections obtained from full (solid lines) and lowest-order (dashed lines) calculations at  $E_d = 11.8$  MeV. Calculations assume the  $S$ -wave Hulthén potential (blue) and the more realistic AV18 NN potential with both  $S$ - and  $D$ -states (black). These are compared to the lowest-order TJ results for the same NN potentials. For the Hulthén potential, the TJ cross sections in next-to-leading order are also shown by the dashed-dotted (magenta) curve.

In the LO limit, the nonlocal potential of Eq. (16) simplifies to

$$\mathcal{U}_{dA}^{(\text{LO})}(R, \mathbf{S}) = \sqrt{4\pi} U_d(R) \sum_{a\alpha} \nu_a(S) (-1)^{a-\alpha} \mathcal{T}_{a-\alpha} Y_a^\alpha(\hat{\mathbf{S}}),$$

where

$$\begin{aligned} \nu_a(S) = 8H(2S) \frac{\hat{J}_d}{\hat{a}} \sum_{l_d l'_d} \hat{l}'_d W(al_d J_d s_d; l'_d J_d) \\ \times \int_0^\infty dx x \tilde{v}_{l'_d a}^{(l_d)}(x, 2S) u_{l'_d}(x). \end{aligned} \quad (23)$$

The central terms ( $a = 0$ ) of this LO nonlocal potential are diagonal in  $L$  with  $\mathcal{U}_{LL'}^J(R, R') = \mathcal{U}_L^J(R, R') \delta_{LL'}$ , and

$$\mathcal{U}_L^J(R, R') = 2\pi U_d(R) \int_{-1}^1 \nu_0(|\mathbf{R} - \mathbf{R}'|) P_L(\mu) d\mu.$$

We have solved the Schrödinger equation for the distorted waves  $\chi_L(R)$  in this limit and then constructed the trivially-equivalent local potentials (TELPs)

$$U_{\text{TELP}}(R) = \frac{R \int dR' R' \mathcal{U}_L(R, R') \chi_L(R')}{\chi_L(R)} \quad (24)$$

which can be compared with the lowest-order adiabatic potentials of the approximation used by Timofeyuk and Johnson (TJ) in Ref. [9]. This comparison, for the  $d-^{40}\text{Ca}$  system at  $E_d = 11.8$  MeV, is shown in Fig. 2. In these and all subsequent calculations we use the non-local nucleon-nucleus potential parameterization of Giannini and Ricco [24], that we denote GR76. We find that the calculated TELP are essentially independent of  $L$  and differ from  $U_{dA}^{\text{loc}}$  by no more than 1% and 2% for the AV18 and Hulthén potentials, respectively. This confirms that, in leading order, the adiabatic potentials can also be obtained from local nucleon potentials by applying an appropriate energy shift. Since this shift is larger when the deuteron  $D$ -state is included, being 67 MeV for AV18, compared to 32 MeV for the Hulthén case, the adiabatic optical potentials should be shallower - as confirmed by the direct calculations shown in Fig. 2a. The cross sections for the  $^{40}\text{Ca}(d,p)^{41}\text{Ca}$  reaction using  $\mathcal{U}_{dA}^{(\text{LO})}$ , shown in Fig. 2b, are also very close to those obtained with  $U_{dA}^{\text{loc}}$  of the TJ approach, given by Eq. (21). Including the  $D$ -state is seen to increase the computed  $(d,p)$  cross sections.

We note that, by making only the LO approximation of Eq. (20) to the full expression for  $\mathcal{U}_{dA}$  (of Eq. (15)) we take into account all corrections beyond the LEA in the TJ derivation of  $U_{dA}^{\text{loc}}$ . However, as was shown in [9], the first-order correction to the LEA involves the fourth power of the (small) nonlocality range parameter  $\beta$ , suggesting this and higher order corrections will be negligible. This expectation is indeed confirmed by our comparisons of  $U_{dA}^{\text{loc}}$  with the exact LO results in Fig. 2.

## V. RESULTS FROM FULL NONLOCAL CALCULATIONS

We now present the results of calculations that compute the exact solutions of the nonlocal integro-differential problem, as given by Eqs. (17) and (18). We note that such solutions could also be approached by systematic development of the higher-order corrections to the LO model of the previous section. For example, for the pure  $S$ -state deuteron case, the next-to-leading order (NLO) corrections were discussed above and in Ref. [8] and, for the Hulthén wave function and the  $^{40}\text{Ca}(d,p)^{41}\text{Ca}$  reaction we have shown that these differ from the exact calculations by  $\approx 3\%$ , see Fig. 2b. However, no such systematic development has yet been carried out when the  $D$ -state is present.

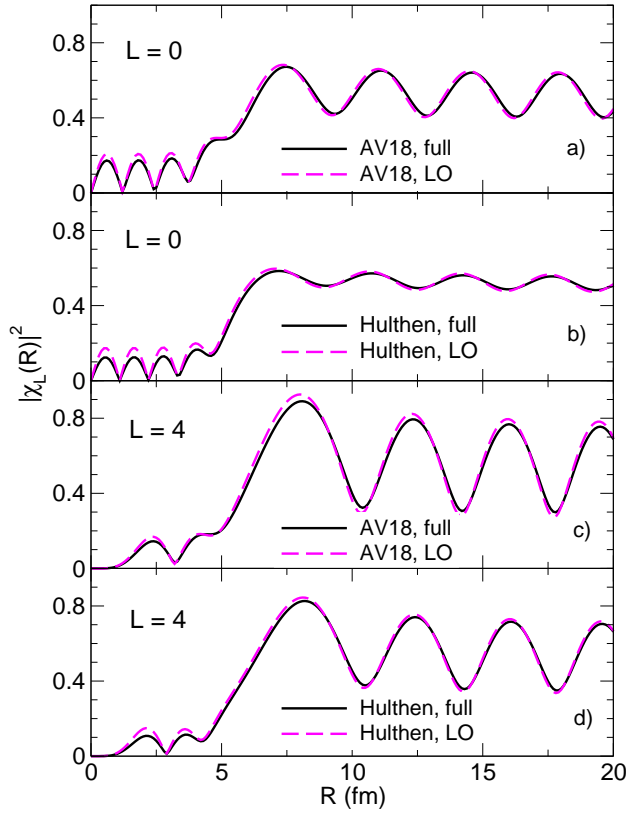


FIG. 3. The  $E_d = 11.8$  MeV,  $d$ - $^{40}\text{Ca}$  distorted waves in  $L = 0$  (a, b) and  $L = 4$  (c, d) partial waves, calculated using the AV18 (a, c) and Hulthén (b, d) NN model potentials. The exact nonlocal calculations are shown by the solid lines while the approximate, lowest-order (LO) calculations are shown as dashed lines.

#### A. Adiabatic distorted waves and tensor force effects

The magnitude of the beyond-LO effects in the exact calculations when the deuteron  $D$ -state is present are assessed in Fig. 3. The deuteron channel partial waves for  $L = 0$  and  $L = 4$  are shown for both the Hulthén and AV18 NN potentials. We note that the wave functions of the full calculations are smaller than the LO results in the nuclear interior, as could be described by a Perey effect. The oscillations of the wave functions obtained with AV18 are also more pronounced, indicative of a reduced deuteron channel absorption. The TELPs deduced from these wave functions are presented in Fig. 2a showing a complicated dependence of their depths and surface diffuseness on both the NN interaction model and the presence of higher-order terms in the presence of the  $D$ -state.

These wave functions and TELPs from the exact calculations include the small contributions from the  $a = 2$  (rank-2 spin-tensor) terms of  $\mathcal{U}_{dA}$ , that generate off-diagonal contributions to the nonlocal potential kernels  $\mathcal{U}_{L'L}^J(R, R')$  and the associated deuteron channel partial

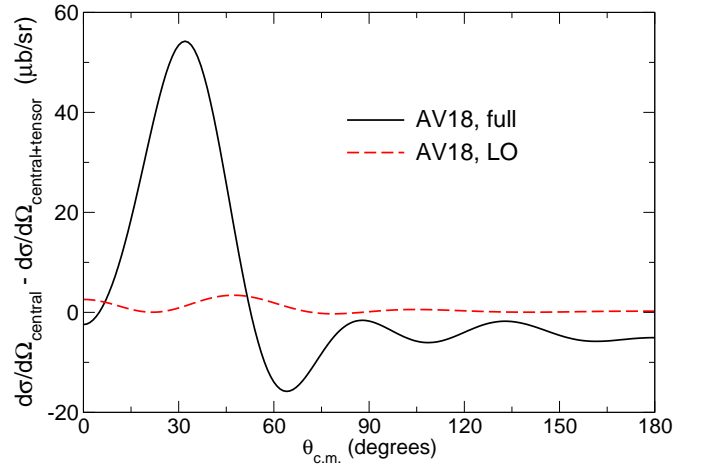


FIG. 4. Difference between the  $^{40}\text{Ca}(d, p)^{41}\text{Ca}$  differential cross sections, for  $E_d = 11.8$  MeV, calculated with only the central terms ( $a = 0$ ) and with the full ( $a = 0, 2$ ) nonlocal adiabatic potential that includes the  $D$ -state generated tensor terms (solid line). The corresponding leading order (LO) potential results are shown by the dashed line.

wave S-matrices  $S_{L'L}^J$ . The latter have maximum values of order  $10^{-2}$  in the cases studied here. These tensor force effects are included fully in the exact distorted wave functions input to the transfer reaction calculations. The importance of these terms, for low energy ( $d, p$ ) reaction cross sections was assessed by comparing calculations that include and neglect the  $a = 2$  contributions to the adiabatic potential. This difference, for the  $^{40}\text{Ca}(d, p)^{41}\text{Ca}$  cross sections, in Fig. 4, is less than  $50 \mu\text{b/sr}$  and represents a change in the calculated differential cross sections of 0.6% or less. Thus, the tensor force effects in the nonlocal  $\mathcal{U}_{dA}$ , arising from the deuteron  $D$ -state, are insignificant for cross-section-based nuclear spectroscopy and astrophysical studies.

#### B. $D$ -state effect on cross sections: transferred orbital angular momentum and separation energy dependence

All calculations above were for the  $^{40}\text{Ca}(d, p)^{41}\text{Ca}(\text{g.s.})$  reaction, carried out in zero-range approximation. The single-particle bound state wave function of the transferred  $1f_{7/2}$  neutron was obtained in the standard potential model description, the Woods-Saxon binding potential having a radius parameter  $r_0 = 1.25$  fm, diffuseness  $a_0 = 0.65$  fm and spin-orbit depth  $V_{SO} = 6$  MeV. Analogous calculations for the  $^{26}\text{Al}(d, p)^{27}\text{Al}$  reaction, populating several final states, were presented in Ref. [16]. As noted there, the magnitude of the cross section changes when using realistic deuteron wave functions, with a  $D$ -state, depends on the details for the final state of the transferred neutron. We now discuss a more systematic study of this observed sensitivity.

As an example we use the  $^{28}\text{Si}(d, p)^{29}\text{Si}$  reaction at



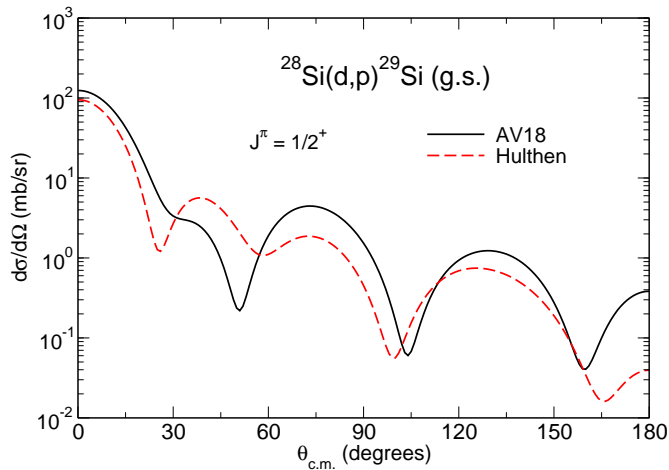


FIG. 5. The  $^{28}\text{Si}(d,p)^{29}\text{Si}(\text{g.s.})$  reaction differential cross sections, at  $E_d = 10$  MeV, obtained using the  $\mathcal{U}_{dA}$  calculated with the  $S$ -state Hulthén and  $S+D$ -state AV18 deuteron wave functions.

$E_d = 10$  MeV,  $^{29}\text{Si}$  having a rich excitation spectrum with low-lying states from several single-particle orbitals. We perform calculations using the GR76 nonlocal nucleon optical potentials and the binding potential geometry stated above. Fig. 5 shows the predicted  $^{29}\text{Si}$  ground-state ( $J^\pi = 1/2^+$ ) differential cross section calculated in the  $S$ -state Hulthén and AV18 deuteron cases. The  $D$ -state is seen to lead not only to an enhanced cross section in the forward peak but also to a modified angular distribution at larger angles. So, changes are complex and not simply a scaling and comparisons with data may depend sensitively on the available range of measured angles.

To explore this cross section  $D$ -state sensitivity further, plus its dependence on the neutron separation energy, we have performed a series of calculations with both the Hulthén and AV18 wave functions. As above, these are for the  $^{28}\text{Si}(d,p)^{29}\text{Si}$  reaction at 10 MeV. Here we have varied the assumed neutron separation energy between 1 to 21 MeV for four assumed transitions of different orbital angular momentum, namely:  $2s_{1/2}$  ( $l = 0$ ),  $2p_{3/2}$  ( $l = 1$ ),  $1d_{3/2}$  ( $l = 2$ ) and  $1f_{7/2}$  ( $l = 3$ ). The fractional changes (as %) in the differential cross sections (at their first peak) of calculations with the Hulthén and AV18 deuteron wave functions are shown in Fig. 6. These ratios depend on the neutron separation energy showing that inclusion of the  $D$ -state can result in cross section changes of up to 30%. The cross section changes for another (fixed) center-of-mass angle are also presented (see caption to Fig. 6) showing that the cross section shapes may also change and that the peak value ratios may not represent an simple overall scaling. In all cases the dependence on the neutron separation energy is significant and changes can reach values of around 50%. Such differences would certainly affect the interpretation of the experimental data in terms of a deduced spectroscopic strength.

### C. Uncertainty of spectroscopic information extracted from $(d,p)$ reactions: $^{26}\text{Al}(d,p)^{27}\text{Al}(7806 \text{ keV})$ case.

To illustrate how including the  $D$ -state in the non-local adiabatic model can affect the spectroscopic factors extracted from  $(d,p)$  reactions, we present calculations of the  $^{26}\text{Al}(d,p)^{27}\text{Al}^*(7806 \text{ keV})$  reaction. The reaction populates the mirror of an astrophysically important state in  $^{27}\text{Si}$ , relevant to the destruction of  $^{26}\text{Al}$  in Wolf-Rayet and Asymptotic Giant Branch stars [25, 26]. The differential cross section for this transition is an (incoherent) combination of  $l = 0$  and  $l = 2$  single-particle transfers; however, only the  $l = 0$  part is important for characterizing the low-energy  $^{26}\text{Al} + p$  resonance in the  $^{27}\text{Si}$  mirror. Spectroscopic factors of  $S_{l=0} = 9.3(19) \times 10^{-3}$  and  $S_{l=2} = 6.8(14) \times 10^{-2}$  were deduced in Ref. [25] from new high-precision data using an analysis that used the ADWA and local global nucleon optical potentials [27]. These calculated cross sections (black curves) and the experimental data are shown in Fig. 7. The figure also shows the cross sections obtained from the present non-local adiabatic model for two choices of NN potential, the pure  $S$ -state Hulthén and the more realistic AV18 potential. All of the calculated  $l = 0$  and  $l = 2$  transfer contributions have been scaled using the spectroscopic factors of Ref. [25] above. The nonlocal model calculations use the same geometries for the neutron bound states potentials as in Ref. [25], with radius parameters  $r_0 = 1.159$  fm and 1.263 fm for the  $l = 0$  and  $l = 2$  states,

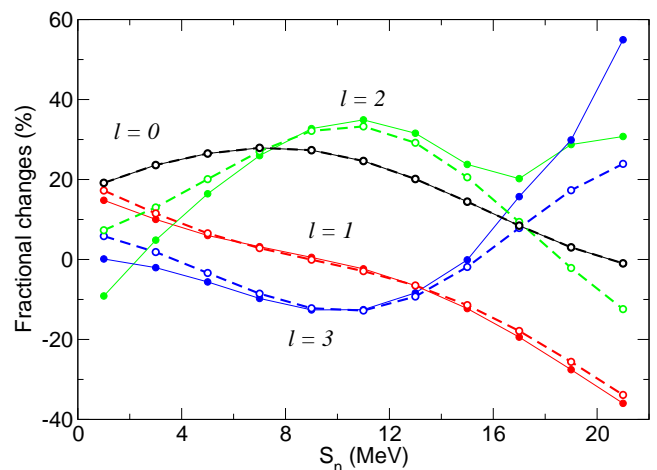


FIG. 6. Fractional changes (as %) in the differential cross sections (at their first peak) of calculations with the Hulthén and AV18 deuteron wave functions (closed circles and solid lines). Results are for the  $^{28}\text{Si}(d,p)^{29}\text{Si}$  reaction. The changes are shown as functions of the assumed separation energy of the transferred neutron with orbital angular momenta  $l = 0, 1, 2, 3$ . The changes in the same cross sections, but at a fixed center-of-mass angle, are also shown (open circles connected by dashed lines). The fixed angles used were 0, 16, 31 and 44 degrees for  $l = 0, 1, 2, 3$ , respectively.



TABLE II. Deduced spectroscopic factors for the  $^{26}\text{Al}(d,p)^{27}\text{Al}$  (7806 keV) reaction from the nonlocal adiabatic potential analyses using different NN potential models. The nonlocal model spectroscopic factors were deduced so as to reproduce the local adiabatic model calculations of Ref. [25], the solid black line in Fig. 7.

	Work of Ref. [25]	Present work			
		Hulthén	AV18	CD-Bonn	RSC
$S_{l=0}$	$9.3(19) \times 10^{-3}$	$8.6(1) \times 10^{-3}$	$8.2(2) \times 10^{-3}$	$9.0(3) \times 10^{-3}$	$8.2(2) \times 10^{-3}$
$S_{l=2}$	$6.8(14) \times 10^{-2}$	$5.8(2) \times 10^{-2}$	$3.3(2) \times 10^{-2}$	$4.5(4) \times 10^{-2}$	$2.8(2) \times 10^{-2}$
$S_{l=0}/S_{l=2}$	0.14	0.15(1)	0.25(2)	0.20(2)	0.29(2)

respectively, diffuseness  $a_0 = 0.7$  fm and a spin-orbit potential depth  $V_{SO} = 6$  MeV.

The summed  $l = 0$  and  $l = 2$  partial cross sections are larger than the experimental data and the earlier local-model calculations and hence the deduced spectroscopic factors from the nonlocal model are smaller. The revised spectroscopic factors from the present nonlocal analyses, fitted so as to reproduce the angular distribution from the local analysis (the black solid curve) are shown in Table II. The errors shown for the nonlocal calculations are those associated with this fit of the different theoretical calculations and do not include the uncertainties associated with the fitting to the data points, shown for the local-model analysis. The spectroscopic factors obtained from analyses using the CD-Bonn [28] and Reid Soft Core (RSC) [29] NN potentials are also tabulated. It was shown in Ref. [16] that these CDB and RSC cross sections essentially provide upper and lower bounds to those calculated with the other NN potentials studied there. One notes that the revised  $S_{l=0}$  are reduced by up to 12% from those of the local potential analysis [25]. Moreover, while the  $S_{l=2}$  obtained with the  $S$ -state Hulthén potential are similar, the reduction can be greater depending on the NN potential choice. Overall, we find this choice introduces an  $\approx 60\%$  uncertainty in the deduced  $S_{l=2}$ , which is significantly larger than the quoted experimental uncertainties. While important for considerations of the structure of  $^{27}\text{Al}$ , this uncertainty does not affect the main conclusion of Ref. [25] - that the  $^{26}\text{Al}(p, \gamma)^{27}\text{Si}$  capture and  $^{26}\text{Al}$  destruction mechanism in novae is dominated by the  $l = 0$  channel.

## VI. CONCLUSIONS

We have extended the nonlocal adiabatic model of  $A(d,p)B$  reactions to include the deuteron  $D$ -state. Whereas adiabatic model deuteron channel potentials generated from local nucleon optical potentials are insensitive to the deuteron  $D$ -state, the nonlocality of the nucleon optical potentials emphasizes the high-momentum parts of the deuteron wave functions in which the  $D$ -state component plays an important role. As a result, the  $(d,p)$  cross sections calculated in the nonlocal adiabatic model are significantly affected by the  $D$ -state component.

We have presented exact calculations of the nonlocal

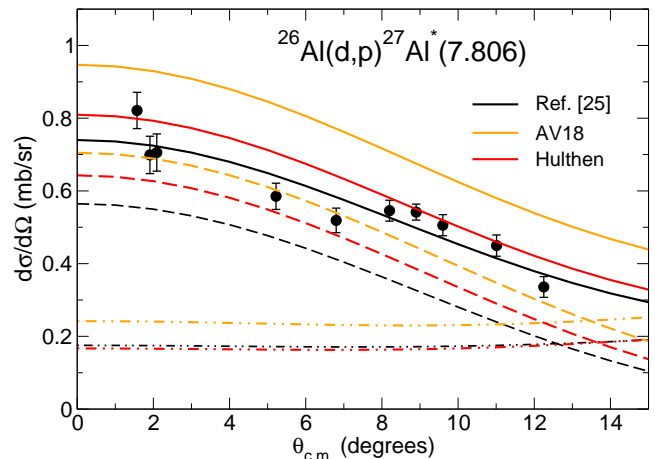


FIG. 7. Calculated  $l = 0$  (dashed lines) and  $l = 2$  (dot-dashed lines) differential cross sections and their sums (solid lines) for the  $^{26}\text{Al}(d,p)^{27}\text{Al}$  (7806 keV) reaction at 12 MeV. The red and orange curves result from nonlocal potential analyses using the Hulthén and AV18 NN wave function models. These calculations have been scaled by the spectroscopic factors deduced from the data using the local potential analysis of Ref. [25], shown by the black lines.

adiabatic model wave functions. To clarify the  $D$ -state dependence we have also performed lowest-order calculations in which the nonlocal nucleon optical formfactors  $U_{NA}$  are evaluated at the  $n - p$  center of mass position. This approximation is shown to generate the leading modifications to the  $(d,p)$  cross sections and to provide insight into the physical picture. Namely, it clarifies that the deuteron channel adiabatic potential can also be generated from local nucleon optical potentials if these are evaluated at energies that are shifted with respect to the usually-used value,  $E_d/2$ . Inclusion of the deuteron  $D$ -state, through the use of realistic NN forces and deuteron wave functions, is shown to increase this energy shift leading to shallower and less absorptive deuteron channel distorting potentials compared to those calculated using a purely  $S$ -state deuteron wave function. Cross sections calculated using this leading order approximation differ from the exact calculations by 12% and 10% for deuteron wave function models with and without a  $D$ -state, respectively.

The degree to which the significant  $D$ -state effects upon the central terms of the deuteron channel interaction affect the  $(d, p)$  cross section magnitudes and angular distributions depend on the transferred angular momentum and the neutron separation energy of the final state. Our calculations show that they can be as large as 50% for some cases and, when two values of  $lj$  are allowed by the selection rules, they add ambiguity to the interpretation of experimental data. For example, when the  $^{26}\text{Al}(d, p)^{27}\text{Al}$  reaction populating the astrophysically-relevant  $^{27}\text{Al}$  (7806 keV) state is analyzed in our nonlocal model, the deduced spectroscopic factors for both  $l = 0$  and  $l = 2$  transfers are reduced. While an analysis without the deuteron  $D$ -state reduces these spectroscopic factors by no more than 16%, inclusion of the  $D$ -state results in a dramatic reduction of the extracted  $l = 2$  spectroscopic strength, by up to a factor of two. The uncertainty associated with different  $S + D$ -state deuteron ground state wave function models is of order 60%. By contrast, the effects of spin-tensor potential terms induced by the deuteron  $D$ -state, even when the nucleon optical potentials are central, are included in the calculated deuteron channel distorted waves and are shown to have negligible effects on the calculated  $(d, p)$  cross sections.

Apart from the  $^{26}\text{Al}(d, p)^{27}\text{Al}$  reaction case, we have presented  $D$ -state results only for the AV18 wave function. The other NN models studied predict smaller  $D$ -state effects [16], so the present results can be considered as a reasonable upper limit. Calculations for  $^{26}\text{Al}$  using the CD-Bonn potential give the smallest  $(d, p)$  cross sections of the models studied and could similarly be considered as a lower limit, but nevertheless show the importance of the  $D$ -state contribution to the spectroscopic factors obtained.

Finally, the present study has used energy-independent nonlocal nucleon potentials. Explicit energy-dependence of the nonlocal nucleon optical potentials, discussed in Ref. [30], may significantly modify model predictions - as was shown in Ref. [31] for the case of a purely  $S$ -state deuteron.

## Appendix: Multipole expansions

The multipole expansion of the nonlocal deuteron channel potential  $\mathcal{U}_{dA}$  in Eq. (16), expressed as a function of the variables  $\mathbf{R}$  and  $\mathbf{S}$ , includes the function  $v_{l_1 l_2}^a(R, S)$  of the radial variables. This is given by the following expression

$$v_{l_1 l_2}^a(R, S) = 8H(2S)\hat{l}_1\hat{j}_d \sum_{l_d l'_d k} (l_1 0 k 0 | l'_d 0) \times \hat{l}'_d \hat{k} W(al'_d l_2 k; l_d l_1) W(al_d J_d s_d; l'_d J_d) \times \int_0^\infty dx x \tilde{v}_{k_1 k_2}^{(l_d)}(x, 2S) \tilde{U}_{l_1}(x/2, R) u_{l'_d}(x). \quad (\text{A.1})$$

Inspection shows that the angular momentum couplings in the second Racah coefficient, with  $J_d = s_d = 1$  and  $l_d, l'_d = 0, 2$ , restrict the spin tensor terms in  $\mathcal{U}_{dA}$  of Eq. (16) to  $a = 0$  (central) and  $a = 2$  (rank-2 tensor) components.

In Eq. (A.1),  $\tilde{v}_{k_1 k_2}^{(l_d)}$  arises from the multipole expansion of the radial components,  $v_{l_d}$ , of the deuteron vertex function,  $V_{np}\phi_0$ , as detailed in and following Eq. (6). Explicitly,

$$\tilde{v}_{k_1 k_2}^{(l_d)}(x, 2S) = \frac{(-1)^{k_2}}{2\langle\phi_0|V_{np}|\phi_0\rangle} \sum_{e, c+d=l_d} \hat{e}^2 \left[ \frac{(2l_d+1)!}{(2c)!(2d)!} \right]^{\frac{1}{2}} \times (c0e0|k_1 0)(d0e0|k_2 0) W(k_1 e l_d d; c k_2) \times x^c (2S)^d \int_{-1}^1 \frac{v_{l_d}(|\mathbf{x} - 2\mathbf{S}|)}{|\mathbf{x} - 2\mathbf{S}|^{l_d+1}} P_e(\mu) d\mu \quad (\text{A.2})$$

with  $\mu = \mathbf{x} \cdot \mathbf{S}/xS$ .

Finally, the  $\tilde{U}_l$  in Eq. (A.1) are the multipoles of the sum the proton and neutron nonlocal potential form factors, i.e.  $\tilde{U}_l(x/2, R) = \tilde{U}_l^n(x/2, R) + \tilde{U}_l^p(x/2, R)$ , where

$$\tilde{U}_l^N(x/2, R) = \int_{-1}^1 d\mu U_{NA}(|\mathbf{x}/2 - \mathbf{R}|) P_l(\mu) \quad (\text{A.3})$$

with  $\mu = \mathbf{x} \cdot \mathbf{R}/xR$ .

## ACKNOWLEDGEMENT

We are grateful to Professor R.C. Johnson for many useful discussions. This work was supported by the United Kingdom Science and Technology Facilities Council (STFC) under Grant No. ST/L005743/1.

- 
- [1] N. Austern, Direct Nuclear Reaction Theories, Wiley, New York, 1970.
  - [2] R.C. Johnson and P.C. Tandy, Nucl. Phys. **A235**, 56 (1974).
  - [3] H. Feshbach, Ann. Rev. Nucl. Sci. **8**, 49 (1958).
  - [4] F. Perey and B. Buck, Nucl. Phys. **32**, 353 (1962).

- [5] F. Perey, Direct interactions and nuclear reaction mechanisms (Gordon and Breach, N.Y. 1963), p.125
- [6] L.J. Titus, F.M. Nunes, Phys. Rev. C **89**, 034609 (2014).
- [7] A. Ross, L.J. Titus, F.M. Nunes, M.H. Mahzoon, W.H. Dickhoff, R.J. Charity, Phys. Rev. **92**, 044607 (2015).
- [8] N.K. Timofeyuk and R.C. Johnson, Phys. Rev. Lett. **110**, 112501 (2013).

- [9] N.K. Timofeyuk and R.C. Johnson, Phys. Rev. C. **87**, 064610 (2013).
- [10] L.J.Titus, F.M.Nunes, G.Potel, Phys. Rev. C **93**, 014604 (2016).
- [11] A. Ross, L.J. Titus, F.M. Nunes, Phys. Rev. C **94**, 014607 (2016).
- [12] A. Deltuva, Phys.Rev. C **79**, 021602 (2009).
- [13] L. Hulthén and M. Sugawara, in Handbuch der Physik, Ed. by S. Flugge (Springer-Verlag, Berlin, 1957), p. 1.
- [14] R.C. Johnson, Nucl. Phys. **A90**, 289 (1967).
- [15] G. Delic and B.A. Robson, Nucl. Phys. **A232**, 493 (1974).
- [16] G.W.Bailey, N.K. Timofeyuk and J.A. Tostevin, Phys. Rev. Lett. **117**, 162502 (2016).
- [17] D.Y. Pang, N.K. Timofeyuk, R.C. Johnson and J.A. Tostevin, Phys. Rev. C **87**, 064613 (2013).
- [18] R.C. Johnson and P.J.R. Soper, Phys. Rev. C **1**, 976 (1970).
- [19] R.B. Wiringa, V.G.J. Stoks and R. Schiavilla, Phys. Rev. C. **51**, 38 (1995).
- [20] R.L. Varner et al, Phys. Rep. **201**, 57 (1991).
- [21] S. Watanabe, Nucl. Phys. **8**, 484 (1958).
- [22] N. B. Nguyen, F. M. Nunes, and R. C. Johnson, Phys. Rev. C **82**, 014611 (2010).
- [23] J.A. Tostevin, University of Surrey version of the code TWOFNR (of M. Toyama, M. Igarashi and N. Kishida) and code FRONT (private communication).
- [24] M.M. Giannini and G. Ricco, Ann. Phys. **102**, 458 (1976).
- [25] V. Margerin, G. Lotay, P. J. Woods, M. Aliotta, G. Christian, B. Davids, T. Davinson, D.T. Doherty, J. Fallis, D. Howell, O.S. Kirsebom, D.J. Mountford, A. Rojas, C. Ruiz, and J.A. Tostevin, Phys. Rev. Lett. **115**, 062701 (2015).
- [26] S. D. Pain, D. W. Bardayan, J. C. Blackmon, S. M. Brown, K. Y. Chae, K. A. Chipps, J. A. Cizewski, K. L. Jones, R. L. Kozub, J. F. Liang, C. Matei, M. Matos, B. H. Moazen, C. D. Nesaraja, J. Okolowicz, P. D. O'Malley, W. A. Peters, S. T. Pittman, M. Ploszajczak, K. T. Schmitt, J. F. Shriner, Jr., D. Shapira, M. S. Smith, D. W. Stracener, and G. L. Wilson, Phys. Rev. Lett. **114**, 212501 (2015).
- [27] A.J. Koning, J.P. Delaroche, Nucl.Phys. **A713**, 231 (2003).
- [28] R. Machleidt, Phys. Rev. C. **63** 024001 (2001).
- [29] R.V. Reid, Ann. Phys. **50**, 411 (1968).
- [30] R.C. Johnson and N.K. Timofeyuk, Phys. Rev. C **89**, 024605 (2014).
- [31] S.J. Waldecker and N.K. Timofeyuk, Phys. Rev. C **94**, 034609 (2016).